Applied Catalysis B: Environmental 127 (2012) 28–35

Contents lists available at SciVerse ScienceDirect

Applied Catalysis B: Environmental

journal homepage: www.elsevier.com/locate/apcatb

A new sight on hydrogenation of F and N-F doped {0 0 1} facets dominated anatase TiO_2 for efficient visible light photocatalyst

Wei Wang, Chunhua Lu*, Yaru Ni, Mingxing Su, Zhongzi Xu

State Key Laboratory of Materials-Orient Chemical Engineering, College of Materials Science and Engineering, Nanjing University of Technology, Nanjing 210009, PR China

ARTICLE INFO

Article history:
Received 3 May 2012
Received in revised form 18 July 2012
Accepted 5 August 2012
Available online 14 August 2012

Keywords:
Ti^{3+}
Visible light photocatalysis
Doping
Oxygen vacancy
{0 0 1} facets

ABSTRACT

Nonmetal doping such by N and F has been studied widely to enhance the visible light photoactivity of TiO_2. Recently, hydrogenation of pure and N doped TiO_2 is also well studied by theoretical calculations. However, little experimental evidence is known about the nature of the hydrogenation effect played on F and N-F doped anatase TiO_2. In this study, hydrogenation of F and N-F doped {0 0 1} facets dominated anatase TiO_2 were prepared by annealing the doped photocatalysts in the 10-bar H_2 atmosphere. Electron paramagnetic resonance (EPR) spectra confirmed the presence of different coordinated Ti^{3+} and oxygen vacancies located in the hydrogenated N and N-F doped TiO_2 as a result of removing the already located N and F species. The visible-light photocatalytic activity of hydrogenated N-F doped TiO_2 was significantly enhanced because of the formation of defect energy state belts and disorder structures. This study gives a new sight on the interaction between H and N, F species in doping TiO_2 and developing efficient visible light photocatalyst by hydrogenation.

1. Introduction

The search for efficient, cheap, nontoxic, and stable photocatalysts for environment protection and improvement have been an increasingly research field in modern times [1,2]. To date, TiO_2 is still one of the most used wide-band-gap semiconductor photocatalysts for a lot of energy and environment applications due to its environment stability, low toxicity, and low cost [3,4]. In order to extend its photoactivity region to the visible and even near infrared range, there have been persistent efforts to modify the band structures of TiO_2 by generating donor or acceptor states through metal and nonmetal doping [5–8]. To date, the incorporation of N has been reported to be the most effective way in enhancing the visible-light photoactivity of TiO_2, even two isolated impurities states which may trap the photo carriers will be formed [9,10]. As is known, different N species can exist within the TiO_2 lattice and they are very stable at temperatures lower than ~600 °C. Recently, H doping, which can improve both the visible light and near infrared light absorption of TiO_2, has been studied by some groups [11,12]. For example, Chen et al. successfully prepared hydrogenated nanophase TiO_2 which extended the light absorption edge to ~1200 nm. They proposed that a disorder state was formed in TiO_2 which further prevented the photogenerated electron and hole's recombination. Through H doping, Ti^{3+} centers which is favorable for light absorption can also be formed within the crystal structures. Based on these studies, N-H doping was proposed to be an efficient method to enhance the visible-light photocatalytic activity of TiO_2 [10,13]. However, most of the studies were based on theoretical calculations which considered that N-H doping can improve the visible light photoactivity of TiO_2 significantly. Experimental evidence, especially to anatase TiO_2, was very scarce. Hoang et al. and Mi et al. [10,14] have made some researches on N-H doped TiO_2. However, the experiments were all conducted with the presence of NH_3, which could not directly illustrate the interaction between N and H introduced by different doping processes.

Recently, {0 0 1} facets dominated anatase TiO_2 nanosheets have also attracted much attention due to the higher reactivity of {0 0 1} facets than the traditional {1 0 1} facets [15]. During the experimental process, F which always serves as morphology control agent was considered can only adsorb on the surface of TiO_2. By the heat treatment above 600 °C or NaOH washing, XPS analysis depicted that the F atoms can be removed completely [16,17]. However, XPS analysis is only sensitive to the surface chemical environment, whether the F influences the inner crystal structures of {0 0 1} facets dominated TiO_2 is still unclear. As is known, F atom can substitute the O atom to produce Ti^{3+} centers, which is similar to H doping. On the other hand, N-F doped TiO_2, which can further improve the visible-light photoactivity of N or F doped TiO_2, have been studied by a lot of research groups [18,19]. Different coordinated Ti^{3+} can be introduced by different methods, such as H doping, F incorporation and vacuum heating [20]. Also, oxygen vacancy will locate

* Corresponding author. Tel.: +86 25 83587252; fax: +86 25 83587220.
E-mail addresses: chhlu@njut.edu.cn, lchnjut@163.com (C. Lu).

0926-3373/$ – see front matter © 2012 Elsevier B.V. All rights reserved.
http://dx.doi.org/10.1016/j.apcatb.2012.08.002

at certain conditions [21,22]. Whether hydrogenation process also plays an positive effect on the crystal structure of F and N-F doped anatase TiO_2 photocatalysts to further improve the visible light photocatalytic activity needs further study.

Herein, our group made a systematic study on hydrogenation of F and N-F doped {0 0 1} facets dominated anatase TiO_2 nanosheets. Different from the previous studies, further hydrogenation of F and N-F doped TiO_2 were conducted in the 10-bar pure H_2 atmosphere. The results demonstrate that the N-F doped {0 0 1} facets dominated anatase TiO_2 becomes an efficient visible light active photocatalyst by further hydrogenation, even N and F could not locate in the TiO_2 lattice together with H. This simple work gives a deeper insight into the H and other nonmetal elements co-doped TiO_2 photocatalysts, which can be extended to develop other highly visible-light-active photocatalysts.

2. Experimental

2.1. Synthesis of F doped {0 0 1} facets dominated TiO_2

All chemicals were used without further purification during the experiment process. The F doped {0 0 1} facets dominated TiO_2 (TiO_2-F) were prepared by a simple hydrothermal method in the light of previously described procedures [21]. Typically, 25 ml of $Ti(OBu)_4$ and 6 ml of HF were added into 9 ml deionized water by sonication and magnetic stirring to produce a homogeneous solution. Then the solution was transferred into a dried Teflon autoclave (60 ml) and kept at 180 °C for 24 h. The as-obtained white product was washed with deionized water and ethanol. Finally, the product was separated by centrifugation and dried in vacuum at 60 °C.

2.2. N doping and hydrogenation process

To introduce N into the TiO_2-F lattice, the pristine product was mixed and grinded with urea (the weight ratio of TiO_2-F to urea was 1/4), and then the mixture was annealed at 400 °C for 2 h in air using a tube furnace to obtain the N-F doped TiO_2 (TiO_2-NF). Hydrogenation of the TiO_2-F and TiO_2-NF were performed using a professional hydrogenation furnace. The furnace was first evacuated and filled with pure H_2 to remove the air several times at room temperature, and then the furnace was filled with pure H_2 to a 10-bar pressure. TiO_2-F and TiO_2-NF were treated in the H_2 atmosphere at 400 °C for 2 h with a temperature ramp rate of 3 °C/min. Finally, the hydrogen treated TiO_2-F (TiO_2-HF) and TiO_2-NF (TiO_2-NHF) were allowed to cool to room temperature naturally.

2.3. Characterization of the photocatalysts

The resulting products were measured on an ARL X'TRA powder X-ray diffraction (XRD) pattern employing Cu Kα radiation. The morphology and structure of as-prepared samples were conducted on a field emission scanning electron microscopy (FESEM) and a JEM-2010 high resolution transmission electron microscopy (HRTEM) with an accelerating voltage of 200 kV. UV–visible diffuse reflectance spectra were obtained using a 3101 spectrophotometer (Shimadzu) with $BaSO_4$ as the reflectance sample. The Fourier transform infrared spectra (FTIR) of as-prepared samples were analyzed with a Vector-22 FTIR spectrometer in the range of 4000–400 cm^{-1}. Electron paramagnetic resonance (EPR) spectra were recorded at 77 K on an EMX 10/12 spectrometer working in the X-band with 100 mg of the sample introduced into an EPR quartz probe cell. Surface composition and chemical environment of the products were analyzed by X-ray photoelectron spectroscopy (XPS) on a PHI5000 VersaProbe system with monochromatic Al Kα X-rays.

2.4. Visible light photocatalytic measurement

In a typical process, 20 mg photocatalyst was suspended in the aqueous solution of the RhB dye (10^{-5} M, 25 ml), which was then placed in a 40 ml cylindrical quartz culture dish under the irradiation of a 500 W xenon lamp fixed with an UV filter to obtain visible light with wavelength beyond 400 nm (Fig. S1 in Supporting information). The xenon lamp was surrounded by the cooling water and was placed 15 cm above the reactor. Prior to the photocatalytic reaction, the suspension was kept in the dark with magnetic stirring for 60 min to establish the adsorption–desorption equilibrium. During the measurement process, 3 ml of the solution was collected at certain time intervals (30 min) to remove the suspended photocatalyst, and the resulting solution was analyzed with the UV-visible spectrophotometer by recording the absorption band maximum (553 nm) of RhB.

3. Results and discussion

3.1. Basic information of the photocatalysts

According to the Wulff structure and the FESEM analysis (Fig. 1a), the two flat and square surfaces in the well-structured pristine particles (TiO_2-F) can be ascribed to the {0 0 1} facets, and the eight isosceles trapezoidal surfaces are the {1 0 1} facets [15,17]. The TiO_2-F side length and thickness are about 100 nm and 15 nm, respectively. A lattice-resolved TEM image collected reveals clear lattice fringes with an interplanar spacing of 0.235 nm, which is consistent with the d-spacing of {0 0 1} facets of anatase TiO_2 (Fig. 1b). This data further demonstrates that TiO_2-F are well-defined by the {0 0 1} facets.

To determine the crystal structure change of as-prepared photocatalysts during the doping process, XRD spectra were collected from the obtained TiO_2-F, TiO_2-NF, TiO_2-HF, and TiO_2-NHF (Fig. 1c). The four samples all give the phase of anatase, indicating no phase change during different doping processes. Further, the diffraction peak intensity increases gradually during the further N doping and hydrogenation processes. Wang et al. and Chen et al. [11,12] have observed a peak intensity decrement during the hydrogenation process, which were ascribed to the increase of defect density in the crystal structure. However, this phenomenon does not appear in the present study. Considering the experimental process, these results may origin from the contest between crystal growth and defect density formation.

As can be seen from Fig. 2a, the optical absorption spectra of the four samples are significantly different. All of them have a nearly overlapped absorption edge, while TiO_2-F almost has no visible light responsibility. In contrast, the onset of the optical absorption edge of TiO_2-NF is extended to around 590 nm, which is the typical optical property of N doped TiO_2. However, a new absorption band up to the infrared range appears in TiO_2-HF and TiO_2-NHF, which means the band structures of TiO_2-F and TiO_2-NF were further modified (narrowed) by hydrogenation. This is similar to the results observed in recent studies on H single doping, while the mechanisms of these doping processes are not very clear [12,14]. In Fig. 2b, the color appearance image of the samples directly depicts the optical absorption spectra change after different doping processes. The bright yellow and dark blue are the typical color of N doped and H doped TiO_2. However, the color (brown) of TiO_2-NHF is very interesting which has not been reported before. This color change must indicate that the crystal structure of TiO_2-NF has changed during the hydrogenation processes.

Enlarged X-ray diffraction peaks of the (1 0 1) plane shown in Fig. 3a depicts that, comparing to TiO_2-F, the center of the diffraction peaks of TiO_2-NF, TiO_2-HF, and TiO_2-NHF moved toward the

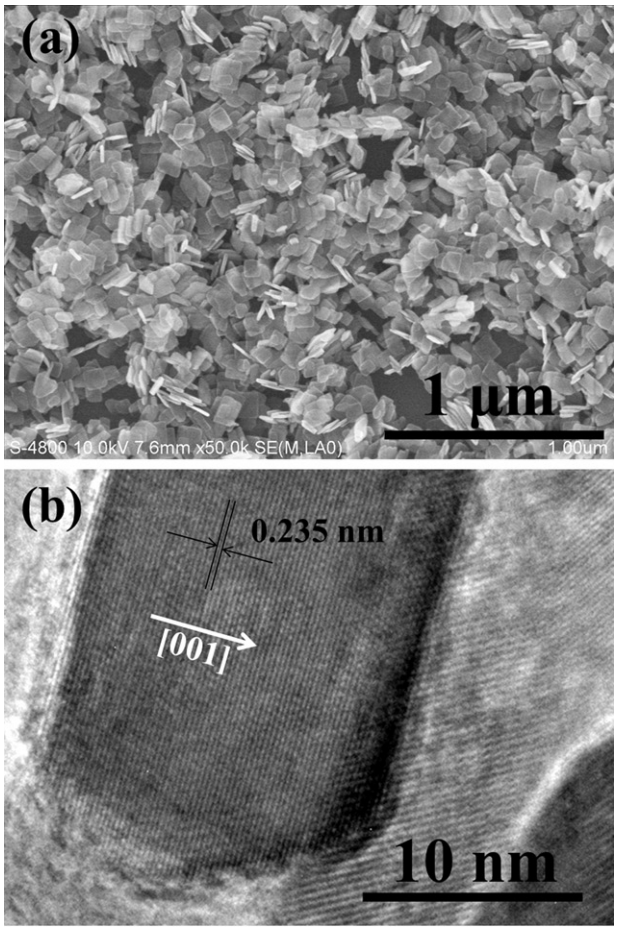

Fig. 1. (a) FESEM image and (b) TEM image of TiO_2-F, and (c) XRD patterns of TiO_2-F, TiO_2-NF, TiO_2-HF, and TiO_2-NHF.

smaller angle range, successively, indicating the expansion of the crystal lattice among the further doped samples. More importantly, the expansion degrees are significantly different. To further prove this point, FTIR spectra of as-prepared photocatalysts were collected. Considerable shifting of Ti—O—Ti stretching frequencies to higher energy, which follows the same rule in the XRD analysis, was observed for TiO_2-NF, TiO_2-HF, and TiO_2-NHF. These types of shifts to higher energies further prove our previous deduction and will be studied systematically.

3.2. EPR and XPS analysis

Low temperature EPR spectra and XPS spectra were recorded to preliminarily investigate the change of the crystal lattice structure.

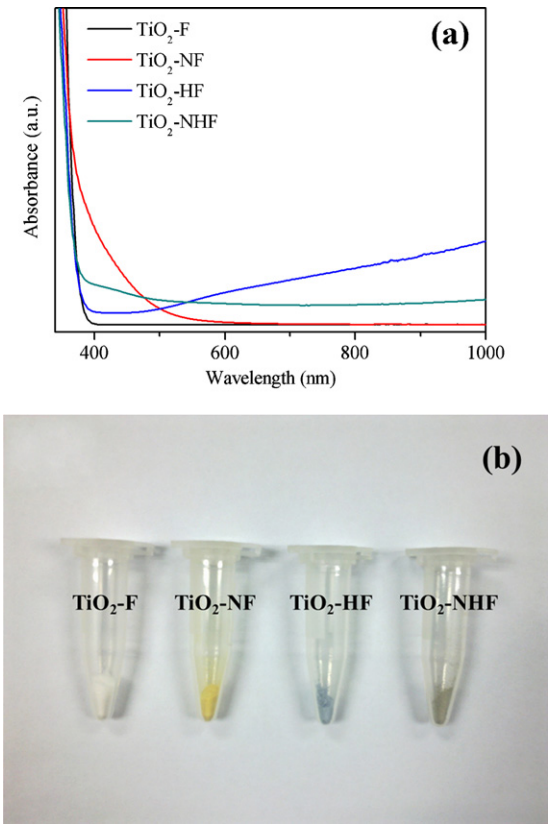

Fig. 2. (a) UV–visible absorption spectra and (b) color appearance of TiO_2-N, TiO_2-NF, TiO_2-HF, and TiO_2-NHF. (For interpretation of the references to color in this figure legend, the reader is referred to the web version of the article.)

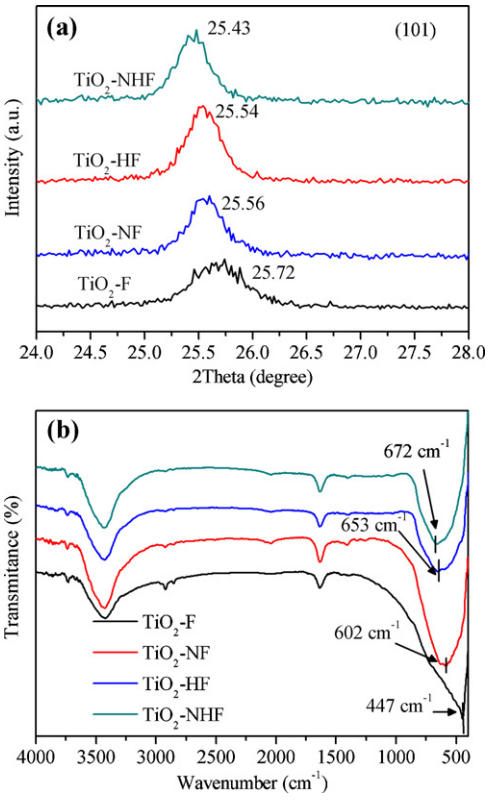

Fig. 3. (a) Enlarged XRD (1 0 1) plane and (b) FTIR spectra of TiO_2-N, TiO_2-NF, TiO_2-HF, and TiO_2-NHF.

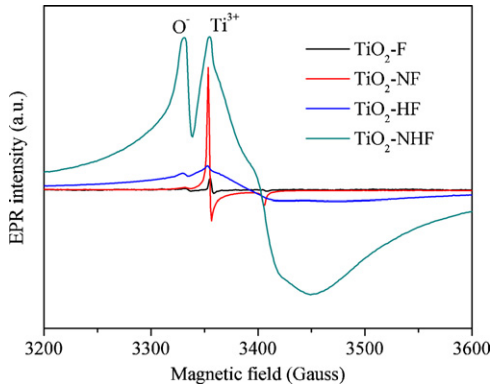

Fig. 4. ESR spectra of TiO_2-N, TiO_2-NF, TiO_2-HF, and TiO_2-NHF.

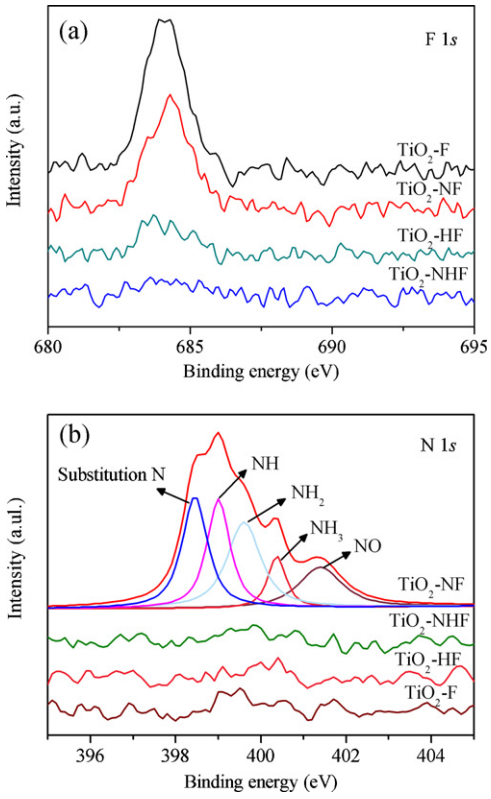

Fig. 5. High resolution (a) F 1s and (b) N 1s XPS spectra of TiO_2-N, TiO_2-NF, TiO_2-HF, and TiO_2-NHF.

As shown in Fig. 4, the four samples show remarkably different EPR signals. Interestingly, a weak EPR signal was detected in TiO_2-F. Since the {0 0 1} facets dominated TiO_2 reported by Yang et al. in 2008, XPS analysis has been used widely and has proved that the F introduced by HF are totally adsorbed on the surface of TiO_2, and no Ti^{3+} was formed for F cannot substitute the O in the TiO_2 lattice during this hydrothermal process [15,21,22]. However, it is clear here that by the EPR analysis, which preserves a high capability in describing paramagnetic defects, a small amount of Ti^{3+}, with g values of $g_{||} = 1.992$ and $g_{||} = 1.962$, was formed in TiO_2-F. This is the typical Ti^{3+} signal of F (substitution) doped TiO_2 [23]. The appearance of Ti^{3+} might because of the inevitably substitution of O atoms by F atoms in the high temperature and high pressure environment which needs further study. After N doping, the intensity of Ti^{3+} signal in TiO_2-NF increases a lot, indicating much more F was incorporated into the TiO_2 lattice to form the Ti—F—Ti chemical bond. Different from the removing of F atoms from the surface by annealing the F-adsorbed samples at 600 °C in air, we obtained more substitution F by annealing the sample at 400 °C [16].

When TiO_2 are thermally treated in the H_2 atmosphere, a fraction of Ti^{4+} ions will be reduced to Ti^{3+} ions, which can be easily detected by the EPR technique [24]. After TiO_2-F and TiO_2-NF were annealed in the 10-bar H_2 atmosphere, a broad signal which can be assigned to Ti^{3+} and a second paramagnetic signal centered at $g = 2.011$ were detected. As is well known, the surface Ti^{3+} may interact with the O_2 to form O_2^- and O^- species, and the g values of them agree with the new paramagnetic signal observed in TiO_2-HF and TiO_2-NHF. However, the signals of O_2^- and O^- are expected to be anisotropic and have components of g tensor closer to 2.00 [25]. We may deduce that the new signal may overlap with the already existed Ti^{3+} signal and thus be invisible, which can be proved by the irregular signal observed in TiO_2-HF and TiO_2-NHF. However, the disappearance of the typical signal g_{zz}, which has a value around 2.02, of O_2^- may allow us to assign the new paramagnetic center with a $g = 2.011$ to the O^- species. Herein, the narrow Ti^{3+} signal in TiO_2-F and TiO_2-NF can be ascribed to the bulk nature of the Ti^{3+} species because no signal of O^- was detected, and this is agree with the results reported before [25]. Considering the Ti^{3+} peak's shape and intensity, we can deduce that the Ti^{3+} presented in TiO_2-HF and TiO_2-NHF is a combination of bulk and surface. However, the Ti 2p XPS spectra (Fig. S2 in Supporting information) do not give any signal of Ti^{3+}, which may because of its limitation in detecting Ti^{3+} [11,26]. A lot of researchers confirmed that the observed broad Ti^{3+} EPR signal in TiO_2-HF and TiO_2-NHF is typical for the reduced TiO_2, while the mechanism is still unclear. We proposed that two reasons may exist. First, it is believed that the concentration of the Ti^{3+} species is in proportion to the detected signal area, and the interaction among the concentrated Ti^{3+} species may broaden the signal. Second, different coordinated Ti^{3+} species may exist. Obviously, the concentration of Ti^{3+} species increases gradually in TiO_2-F, TiO_2-NF, TiO_2-HF, and TiO_2-NHF. More importantly, the O^- signal in TiO_2-NHF is very strong compared to the others.

To get a deeper insight into the structure change by further modification, XPS analysis was given. Although XPS technique was very sensitive to the surface chemical environment, it is still very important and can be used to investigate the change of the element chemical environment. The high resolution XPS spectra of F 1s (Fig. 5a) shows that a single peak with the maximum centered at a binding energy of 684.3 eV is observed for TiO_2-F. According to the former reports, this peak can be associated with the surface fluorination [27,28]. However, Yu et al. observed an F 1s XPS peak with a higher binding energy (688.3–688.6 eV) which was ascribed to the substitution F in their studies. This signal was not detected in the present analysis which may be attributed to different experiment method and has been reported before [23]. After further N doping and hydrogenation treatment, the signal intensity changes a lot. In the photocatalyst of TiO_2-NF, the total F detected decrease a little, some of them may move inside the TiO_2 lattice to substitute the O atoms resulting in a higher EPR intensity, while some of them may be removed by calcination for surface F can be removed by calcining at 600 °C. After H_2 treatment, the signal of TiO_2-F further decreased. If the disappeared F was moved into the TiO_2 lattice to form the Ti—F—Ti chemical bond, a stronger EPR signal similar to the one detected in TiO_2-NF must existed. However, a broad signal with a lower intensity was detected instead. Considering the signal detected in TiO_2-NHF, which gives no peak of F, we may deduce that all the F atoms were taken away by the H_2 treatment in the form of HF gas.

Further, the XPS spectra of N 1s was analyzed (Fig. 5b). A complicated signal of N is observed in TiO_2-NF, while the rest three samples give no signal of N at all. The N species exist in the N doped TiO_2 is still under debate because a lot of different signals have

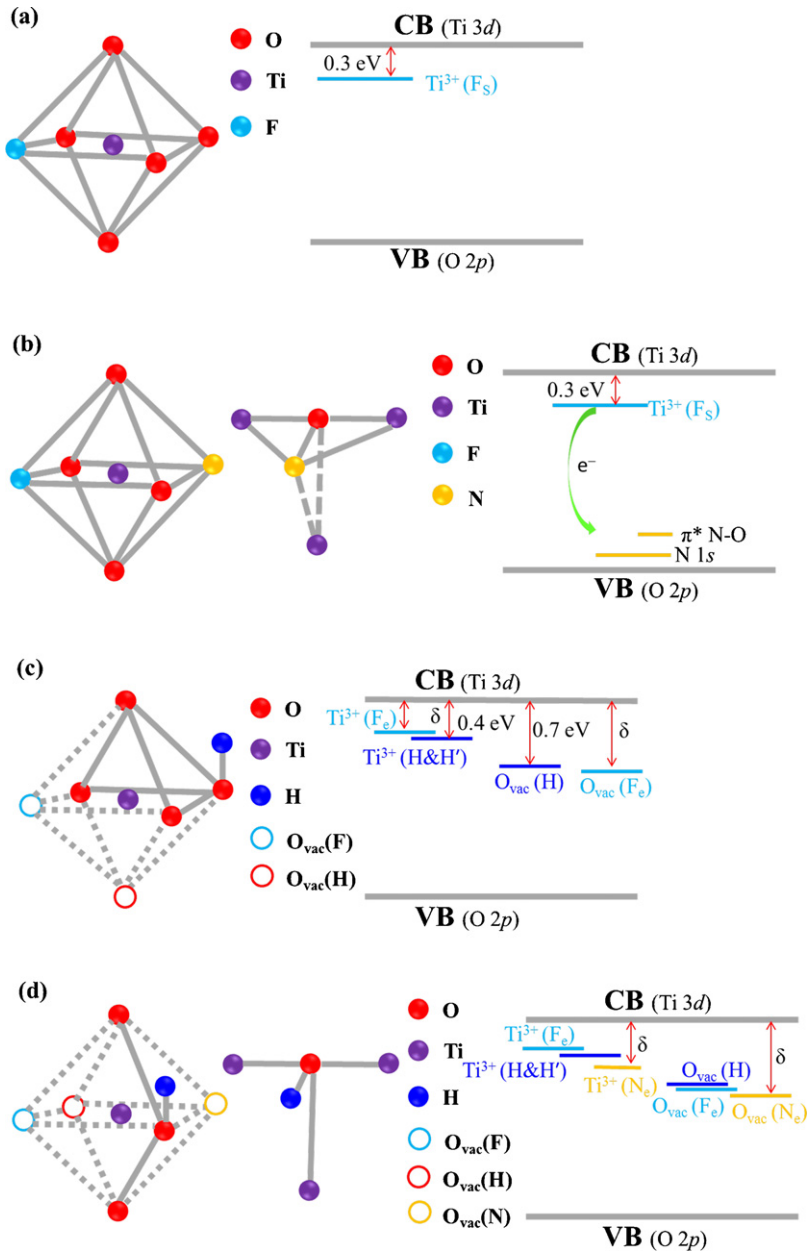

Fig. 6. Schematic illustration of the crystal structure change and defect states formation of (a) TiO_2-N, (b) TiO_2-NF, (c) TiO_2-HF, and (d) TiO_2-NHF.

been detected in the former studies [29,30]. Now it is convinced that the N signal presented is based on the experiment methods and processes. Considering our experiment process, the N 1s signal appeared in TiO_2-NF can be assigned to substitution N and intersectional N. Urea will decompose into NH_3 and CO_2 at 400 °C, and the NH_3 is the compound that modified TiO_2. According to the previous studies, the intersectional N may exist in the TiO_2 lattice in the form of NH, NH_2, NH_3 and NO_x [31]. Whatever the N species even it is bonded to H, they all disappeared after treated in the 10-bar H_2 atmosphere. N modified TiO_2 has been studied for nearly 12 years since 2001 reported by Asahi et al. It is believed that the N doped TiO_2 is very stable and the N species located in the TiO_2 lattice cannot be removed at the temperature lower than ~600 °C. During our experiment process, a smelly NH_3 overflowed when we open the reactor containing the sample of TiO_2-NHF. More importantly, the color (brown) of TiO_2-NHF is different from the typical color (bright yellow) of N doped TiO_2. Even though there have been a lot of calculation researches on N-H doping [13,26,32]. However, it is proved here that this doping effect cannot happen, at least in our experimental environment. It is also reported that H_2 treated TiO_2 will form oxygen vacancy in the lattice, for H_2 will interact with the O atom to form H_2O [26]. Considering the similar chemical properties of N, O, and F, the N species together with the F atoms located must have been removed from the TiO_2 lattice.

3.3. *Visible light photoactivity and mechanisms*

Schematic illustrate of the aforementioned doping process are shown in Fig. 6. As there is very scare study on hydrogenation of F and N-F doped anatase TiO_2, some of the data in the band structure correlating to Ti^{3+} are referred to the paper published by Di Valentin et al. [26], and the unclear data is shown as δ. In TiO_2-F, only a small amount of F atoms substitute the O atoms, resulting in mild n-type doping. In this case, an extra electron in the lattice will reduce Ti^{4+}

to $Ti^{3+}(F_s)$ (s = substitution), which is well coordinated. Herein, only a small distortion of the TiO_2 lattice will happen. The calculation worked by Czoska et al. and Di Valentin et al. [23,26] depicts that the lattice will be slightly expanded.

When N was incorporated into the lattice, various N species will exist in the lattice. Mi et al. [10] claimed that when N was introduced, there will be two isolate N 2p states above the valence band. Pan et al. [13] reported that the incorporation of intersectional N will push the oxygen atom away from its original position, leading to the extension of Ti—O bonds. However, the substitutional N makes little local structure distortion of anatase TiO_2 structure. In the present study, a large amount of N was incorporated into TiO_2-F. It is obvious that the structure distortion caused by N and F incorporation is more serious than that caused by F single incorporation. One more thing, there will be a reversible electron transfer between the $Ti^{3+}(F_s)$ energy level and the paramagnetic N centers. This effect can explain why no EPR signal of N species was detected, which has been first reported by Livraghi et al., proved by Napoli et al. and Hoang et al. [14,33,34].

For the photocatalyst of TiO_2-HF, the H_2 will react with the O and F atom, resulting in the formation of H_2O and HF which will escape from the TiO_2 lattice [11]. Thus the $O_{vac}(H)$ and $O_{vac}(F_e)$ (e = escape) introduced by H_2 was formed. On the other hand, the H prefers to bond perpendicular to the Ti—O—Ti plane in the anatase TiO_2, which will result in H^+ bound to a lattice oxygen and an extra electron, which will located on the Ti^{4+} to produce a new kind of $Ti^{3+}(H')$ [13]. Also, $Ti^{3+}(F_e)$ and $Ti^{3+}(H)$ related to $O_{vac}(F_e)$ and $O_{vac}(H)$ will happen. Thus, the crystal lattice may change a lot. As shown in the XRD and FTIR analysis, the lattice distortion introduced by hydrogenation seems much more serious than that by N-F incorporation, indicating that the crystal lattice is much more disordered.

Similarly, there will be an interaction between the H_2 and the N, F, and O atoms in TiO_2-NHF. The optimized bond length of N-H in the N doped TiO_2 is very similar to that in NH_3, so it can be well deduced that NH_3 will be formed when the N modified TiO_2 was presented in the H_2 atmosphere [10]. However, the 10-bar gas pressure may be an important factor that removes the N and F from the TiO_2 lattice completely, which need further study. As a result, different oxygen vacancies, such as $O_{vac}(N_e)$, $O_{vac}(F_e)$, and $O_{vac}(H)$, were formed as a result of the H doping and the escape of N and F atoms. Naturally, corresponding $Ti^{3+}(N_e)$, $Ti^{3+}(F_e)$, $Ti^{3+}(H)$ and $Ti^{3+}(H')$ are formed. Further, the EPR analysis gives very strong signal assigned to $O^-$and Ti^{3+}, proving the above analysis. The O 1s XPS spectra (Fig. S3 in Supporting information) show a significant change of the O chemical environment in TiO_2-NHF, while the rest photocatalysts remain almost the same. This result is very different from the results reported before [10,13]. Hoang et al. recently reported that after placed the rutile TiO_2 nanowire in the H_2 and NH_3 atmosphere, successively, N-H doped TiO_2 was obtained. This result can be ascribe to the final doping process was performed in the NH_3 atmosphere, which originally possesses the N-H interaction.

It is well-known that the RhB is one of the most important organic dyes that have been used widely, which often results in environment contamination. Herein, we choose RhB to evaluate visible light photoactivity of the prepared photocatalysts. Before the photocatalysis, the solution containing the photocatalyst and RhB was magnetic stirred in the dark to establish the adsorption–desorption equilibrium, and the RhB concentration measured here is regarded as the initial concentration (C_0). Blank test without the photocatalyst is also conducted for RhB will decompose slowly under light irradiation. The as evaluated photocatalytic results are shown in Fig. 7. The results show that TiO_2-NHF gives the highest visible light photocatalytic activity, while the photocatalytic ability of TiO_2-NF and TiO_2-HF are similar to each

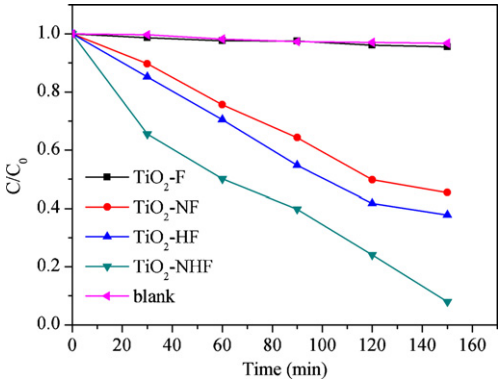

Fig. 7. Photocatalytic activities of TiO_2-N, TiO_2-NF, TiO_2-HF, and TiO_2-NHF under visible light irradiation beyond 400 nm.

other. In contrast, blank test and TiO_2-F almost exhibit no ability to decompose RhB under visible light irradiation, which may result from that only a small amount of Ti^{3+} is formed in TiO_2-F. This result may also relate to the amount of O^- and Ti^{3+}, which influences the band structures significantly, detected in the EPR analysis.

The valance band XPS spectra are presented in Fig. 8a to investigate the band structures of the different doped TiO_2. It is clear that TiO_2-F, TiO_2-NF, and TiO_2-HF have similar band edge position of ~2.64 eV. For the hydrogenated TiO_2 nanowire arrays reported by Wang et al. [11], the band edge position was the same with the pristine sample. Also, as the best of our knowledge, the N, F, and N-F doped TiO_2 also give little change in the band edge position. The enlarged band edge spectra (Fig. 8b) clearly depicts that the band edge position of TiO_2-NHF shifts to ~2.36 eV, and a shoulder with an edge at ~1.85 eV is observed. This may result from a large amount of O_{vac} and Ti^{3+} were formed in the band gap. When a low

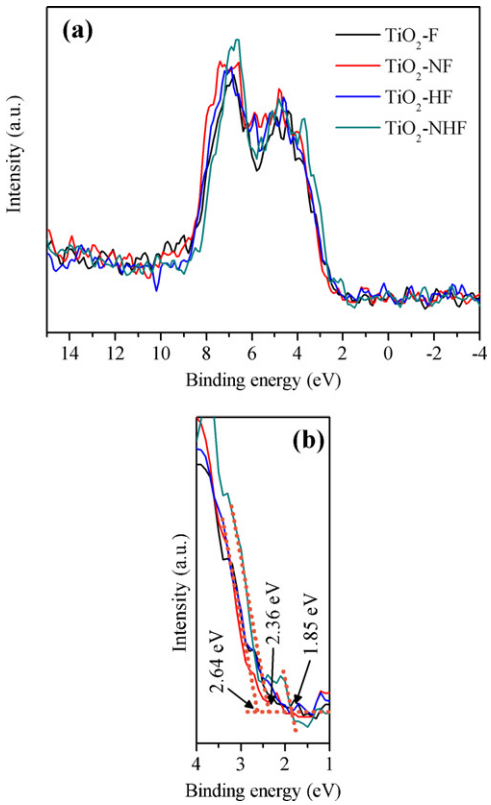

Fig. 8. (a) XPS valence band spectra and (b) band edge position of TiO_2-N, TiO_2-NF, TiO_2-HF, and TiO_2-NHF.

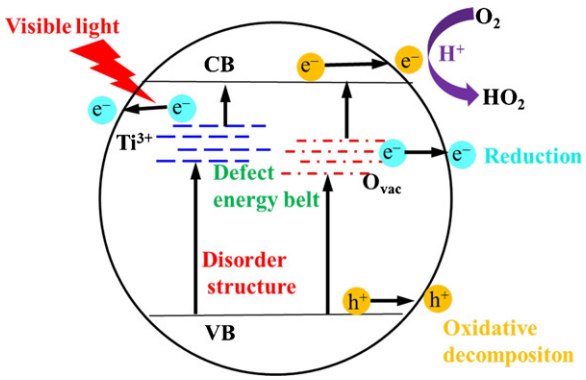

Fig. 9. The schematic illustration of the band structure and visible light photocatalytic process of TiO_2-NHF.

quantity of Ti^{3+} and O_{vac} are formed, they only form some isolate defect energy levels in the band gap, which are just like the isolated energy levels introduced by N doping. These defect levels enhance the light absorption of the photocatalysts, but they also serve to trap the photo carriers, too. This may be the reason why TiO_2-NF and TiO_2-HF gives similar visible light photocatalytic activities. For the hydrogenated N-F doped TiO_2, a large amount of different coordinated Ti^{3+} and oxygen vacancies are exist in the crystal lattice, they will form a wide defect energy state belt which not only truly narrow the band gap and significantly enhance the light absorption but also facilitate the photo carriers' migration. Recently, Chen et al. [12] attribute the band gap modification to the disorder state presented on the surface of nanophase TiO_2. In the valence band spectra, they also observed a small shoulder, just as the signal we observed in the present study. In TiO_2-NHF, the atoms' incorporation and escape distorted the TiO_2 lattice significantly. This will also form a disorder structure inside the TiO_2 crystal, as proved by the XRD and FTIR analysis. Herein, the shoulder appeared at ~1.85 eV may attribute to the disorder state existed in TiO_2, which is just like what Chen et al. reported. As a result, a truly existed defect energy state belt related to different Ti^{3+} and O_{vac} and a disorder structure are important factors for efficient band gap narrowing and visible light photoactivity enhancement of TiO_2-NHF. The schematic illustration of the band structure and visible light photocatalytic process of TiO_2-NHF are shown in Fig. 9.

4. Conclusion

In summary, we made a systematic study on the hydrogenation of N and N-F doped anatase {0 0 1} facets dominated anatase TiO_2. A small amount of F atoms would modify the TiO_2 during the hydrothermal process, resulting in $Ti^{3+}(F_s)$. After N doping, the visible light absorption of TiO_2-NF was enhanced, and much more F atoms substituted the O atoms which further improve the $Ti^{3+}(F_s)$ quantity. When TiO_2-F and TiO_2-NF were presented in the 10-bar H_2 atmosphere, the light absorption ability was extended to the infrared range. More importantly, the experiment results showed that N-H and N-H-F doped TiO_2 were not obtained. Instead, the located F and N atoms escaped from the crystal lattice in the form of HF and NH_3. As a result, a large amount of different coordinated oxygen vacancies ($O_{vac}(F_e)$, $O_{vac}(N_e)$, $O_{vac}(H)$) and Ti^{3+} ($Ti^{3+}(F_e)$, $Ti^{3+}(N_e)$, $Ti^{3+}(H)$, and $Ti^{3+}(H')$) were formed in TiO_2-NHF, resulting in a wide defect energy state belt which would not trap the photo carriers and a serious disorder structure. Thus the band gap of TiO_2-NHF was truly narrowed and the visible light photoactivity was enhanced significantly. This simple experiment gives a new sight into the mechanism of H combined other nonmetal elements co-doped TiO_2, which can be extended to apply other doping process to develop new photocatalysts with high visible light photocatalytic activity.

Supporting information

Visible light spectrum used for photocatalytic measurement (Fig. S1), XPS spectra of Ti 2p (Fig. S2), and XPS spectra O 1s (Fig. S3).

Acknowledgements

This work was supported by the Innovation Foundation for Graduate Students of Jiangsu Province China (CXLX11_0346) and a project funded by the Priority Academic Program Development of Jiangsu Higher Education Institutions. The authors also thank Yunfeng Zhu of Nanjing University of Technology for hydrogenation treatment.

Appendix A. Supplementary data

Supplementary data associated with this article can be found, in the online version, at http://dx.doi.org/10.1016/j.apcatb.2012.08.002.

References

[1] X. Chen, S. Shen, L. Guo, S.S. Mao, Chemical Reviews 110 (2010) 6503–6570.
[2] S.U.M. Khan, M. Al-Shahry, W.B. Ingler, Science 297 (2002) 2243–2245.
[3] R. Leary, A. Westwood, Carbon 49 (2011) 741–772.
[4] A. Fujishima, X. Zhang, D.A. Tryk, Surface Science Reports 63 (2008) 515–582.
[5] S. Bingham, W.A. Daoud, Journal of Materials Chemistry 21 (2011) 2041–2050.
[6] H. Wang, Z. Wu, Y. Liu, Journal of Physical Chemistry C 113 (2009) 13317–13324.
[7] G.X. Cao, Y.G. Li, Q.H. Zhang, H.Z. Wang, Journal of the American Ceramic Society 93 (2010) 1252–1255.
[8] A. Kachina, E. Puzenat, S. Ould-Chikh, C. Geantet, P. Delichere, P. Afanasiev, Chemistry of Materials 24 (2012) 636–642.
[9] R. Asahi, T. Morikawa, T. Ohwaki, K. Aoki, Y. Taga, Science 293 (2001) 269–271.
[10] L. Mi, P. Xu, H. Shen, P.-N. Wang, W. Shen, Applied Physics Letters 90, 171909 (2007) 1–3.
[11] G. Wang, H. Wang, Y. Ling, Y. Tang, X. Yang, R.C. Fitzmorris, C. Wang, J.Z. Zhang, Y. Li, Nano Letters 11 (2011) 3026–3033.
[12] X. Chen, L. Liu, P.Y. Yu, S.S. Mao, Science 331 (2011) 746–750.
[13] H. Pan, Y.-W. Zhang, V.B. Shenoy, H. Gao, Journal of Physical Chemistry C 115 (2011) 12224–12231.
[14] S. Hoang, S.P. Berglund, N.T. Hahn, A.J. Bard, C.B. Mullins, Journal of the American Chemical Society 134 (2012) 3659–3662.
[15] H.G. Yang, C.H. Sun, S.Z. Qiao, J. Zou, G. Liu, S.C. Smith, H.M. Cheng, G.Q. Lu, Nature 453 (2008) 638–641.
[16] J.G. Yu, L.F. Qi, M. Jaroniec, Journal of Physical Chemistry C 114 (2010) 13118–13125.
[17] G. Liu, H.G. Yang, X. Wang, L. Cheng, H. Lu, L. Wang, G.Q. Lu, H.-M. Cheng, Journal of Physical Chemistry C 113 (2009) 21784–21788.
[18] C. Di Valentin, E. Finazzi, G. Pacchioni, A. Selloni, S. Livraghi, A.M. Czoska, M.C. Paganini, E. Giamello, Chemistry of Materials 20 (2008) 3706–3714.
[19] S. Livraghi, K. Elghniji, A.M. Czoska, M.C. Paganini, E. Giamello, M. Ksibi, Journal of Photochemistry and Photobiology A: Chemistry 205 (2009) 93–97.
[20] T.L. Thompson, J.T. Yates, Chemical Reviews 106 (2006) 4428–4453.
[21] X. Han, Q. Kuang, M. Jin, Z. Xie, L. Zheng, Journal of the American Chemical Society 131 (2009) 3152–3153.
[22] H.G. Yang, G. Liu, S.Z. Qiao, C.H. Sun, Y.G. Jin, S.C. Smith, J. Zou, H.M. Cheng, G.Q. Lu, Journal of the American Chemical Society 131 (2009) 4078–4083.
[23] A.M. Czoska, S. Livraghi, M. Chiesa, E. Giamello, S. Agnoli, G. Granozzi, E. Finazzi, C.D. Valentin, G. Pacchioni, Journal of Physical Chemistry C 112 (2008) 8951–8956.
[24] R.F. Howe, M. Gratzel, Journal of Physical Chemistry 91 (1987) 3906–3909.
[25] J. Strunk, W.C. Vining, A.T. Bell, Journal of Physical Chemistry C 114 (2010) 16937–16945.
[26] C. Di Valentin, G. Pacchioni, A. Selloni, Journal of Physical Chemistry C 113 (2009) 20543–20552.
[27] J.C. Yu, J.G. Yu, W.K. Ho, Z.T. Jiang, L.Z. Zhang, Chemistry of Materials 14 (2002) 3808–3816.
[28] H. Park, W. Choi, Journal of Physical Chemistry B 108 (2004) 4086–4093.

[29] M. Ceotto, L. Lo Presti, G. Cappelletti, D. Meroni, F. Spadavecchia, R. Zecca, M. Leoni, P. Scardi, C.L. Bianchi, S. Ardizzone, Journal of Physical Chemistry C 116 (2012) 1764–1771.
[30] O. Diwald, T.L. Thompson, T. Zubkov, S.D. Walck, J.T. Yates, Journal of Physical Chemistry B 108 (2004) 6004–6008.
[31] Y.K. Kim, S. Park, K.-J. Kim, B. Kim, Journal of Physical Chemistry C 115 (2011) 18618–18624.
[32] X. Han, G. Shao, Journal of Physical Chemistry C 115 (2011) 8274–8282.
[33] S. Livraghi, M.C. Paganini, E. Giamello, A. Selloni, C. Di Valentin, G. Pacchioni, Journal of the American Chemical Society 128 (2006) 15666–15671.
[34] F. Napoli, M. Chiesa, S. Livraghi, E. Giamello, S. Agnoli, G. Granozzi, G. Pacchioni, C. Di Valentin, Chemical Physics Letters 477 (2009) 135–138.